Modeling Linear Free Radical Copolymerization by Digital Encoding

Rima Y. Tabash,[†] Fouad A. Teymour,*[,†] and Jon A. Debling[‡]

Department of Chemical and Environmental Engineering, Illinois Institute of Technology, Chicago, Illinois 60616, and Johnson Polymer, 8310 16th Street, PO Box 902, Sturtevant, Wisconsin 53177-0902

Received June 30, 2005; Revised Manuscript Received November 12, 2005

ABSTRACT: Copolymer chains are characterized by chain length, chain composition, and sequence length distributions. Despite the wealth of information these distributions provide, they are incapable of determining the microstructure and concentration of individual chain types along the conversion path at the level of "*polymeric isomers*", which are chains of same length and composition but have different monomeric sequences. This work is intended to develop the mathematical equations of "*digital encoding of polymer chains*", which is a technique that encapsulates all the information about polymer chain architecture in a unique descriptive manner and is capable of determining the concentrations of all polymer chain types and their isomers. Two types of histograms can be generated: the encoded sequence length distribution (SLD) and the chain type distribution (CTD), which enable a specific visualization of results.

Introduction

Polymeric materials have had a significant impact on the development of modern technologies that is pushing researchers in the polymer field to face a greater challenge and invest increased efforts in developing unprecedented materials that can add to and/or cope with the rapid technological advancements of the new millennium. This is a result of the successful use of polymers, with their diverse properties, in a variety of applications.

A polymer is typically produced as a collection of molecules (chains) that differ in molecular weight, molecular formula, composition, and structure. On the contrary, small molecule materials are usually utilized in high-purity forms or in well-defined blends and mixtures. Though polymers possess a distributive nature that is advantageous for many applications, one can argue that some applications benefit only from the properties contributed by a subgrouping of chains present in a polymer sample, while other chains could either be totally uninvolved or actually lessening the magnitude of display of the desired property. There must then exist another end for the spectrum at which high-purity polymeric components have an untapped potential to provide previously unobserved novel properties beyond the capabilities of presently known polymeric materials. It is conceivable that the ultimate achievement of this level of specificity in producing or purifying polymers will drive the polymer industry into more advanced innovations.

Before this can be achieved, however, new methods had to be developed to enable the description of polymeric chains at such a specific level and, equally important, to overcome the last long impediment in describing the concentration of individual polymer chains along the conversion path which left researchers with no choice but to turn to statistical methods to describe the copolymer composition and sequence length distributions.

Thus, the motivation of this work derives from the recent introduction, by Debling and Teymour[1] in 2002, of a modeling methodology, termed "*digital encoding of polymer chains*", that is capable of describing copolymer molecules not only at the chain length and composition levels but also down to the distinction of the specific monomer sequencing on these chains. They proposed the concept of "*polymeric isomers*", which are polymer molecules of the same chain length, composition, and molecular formulas, but have different monomeric sequences and can vastly differ in their properties in the same manner customary to small molecule materials.

The digital encoding technique utilizes concepts from genetic engineering, symbolic dynamics, and information theory. It is analogous to the precise linear sequence coding of the bases along a DNA molecule which is ultimately responsible for the linear sequence of amino acid residues in a particular protein with a specific activity.[2] It is also similar to approaches in the analysis of chaos[3−5] and in signal processing[6,7] where in these approaches streams of data are digitized according to their location with respect to the data mean, e.g., 0 = below and 1 = above, or to a number of prespecified regions. The statistics of sequence of *n* consecutive data points are then analyzed to detect whether the signal is behaving in a random or structured fashion. Such information is useful for developing system diagnostics and compare computational models with experiments.

The digital encoding technique involves replacing distinguishable features of the chain such as monomer units, branches, functionality, etc., with a number. Then the unique sequence of these numbers provides a digital code, which, depending on the base of the arithmetic utilized (binary, ternary, etc.), can be translated into a unique decimal equivalent to be used in the computation of polymer isomer histograms and the visualization of results.

The novelty of this method lies in its ability of presenting any polymer chemistry with a digitized notation that is mathematically based, highly descriptive, and yet amenable to modeling. These collective qualities allow unlimited possibilities of application ranging from representing the different copolymerization chemistries and models, relearning, to reevaluating these models for various systems and under different conditions. Relearning about these systems includes the redetermination of reactivity ratios, better discrimination of the proposed models, analysis of termination modes, and the application of control policies to overcome the compositional drift in dynamical systems.

* Corresponding author: Tel 312-5678947; Fax 312-5678874; e-mail teymour@iit.edu.
[†] Illinois Institute of Technology.
[‡] Johnson Polymer.

10.1021/ma051417y CCC: $33.50 © 2006 American Chemical Society
Published on Web 12/24/2005

Another application is in the determination of the microstructure of a novel class of materials called gradient copolymers and its structure−property relationship. This class of copolymers has a tapered composition of two monomers arranged along the polymer chain. Such well-defined structure can be synthesized by controlled/living radical polymerization methods.[8−14] Simulations[8−11] of the interfacial effects of immiscible polymers modified by the addition of gradient copolymers indicate that gradient copolymers can be used as compatibilizers, surfactants, and novel materials for vibration and noise damping.

In this work, the theoretical basis and detailed modeling equations of the digital encoding technique are presented for a copolymerization process obeying the terminal model in a steady-state isothermal continuous stirred tank reactor (CSTR). The sequence length distribution (SLD) concept is revisited, and SLD histograms are redesigned to include the statistics of polymeric isomers. The concentrations of these polymeric isomers are then calculated and presented in what we term "chain type distribution" (CTD), which was not previously possible. The methodology is applied to systems at various kinetic and process conditions including a case study of styrene/methyl methacrylate to discriminate between copolymerization propagation and termination mechanisms and the potential of differentiating between kinetic parameters. Finally, the model results are analyzed to detect any regularities or patterns in the behavior of the system by calculating the modified Shannon entropy.[15] Such patterns, if they exist, serve as a proof that copolymer microstructure evolves deterministically and that short chains are representative of the copolymerization system and even contain more information, compared to that supplied by long chains, which can be unfolded to better understand the copolymerization kinetics.

Digital Encoding Technique

We will consider a copolymerization scheme involving two monomers and assign a number "0" to the first, M_0, "1" to the second, M_1, and thus use the binary mathematics to denote the chain architecture. Once a binary string is generated, a numerical representation of the specific sequence of monomers is achieved by converting the binary code into a decimal equivalent (d). This allows for a better display of the statistics and more effective characterization of observed patterns through the sequence histograms. Note that there is no restriction to using the binary mathematics but rather the arithmetic base can be raised to ternary or more depending on how many polymer chain features are desired to be described beside the monomer units, such as branching, functionality, double bondings, etc. In all cases, the base of the arithmetic used is denoted by (b).

As the main objective is to provide distinction at the level of polymer chains as well as at the monomer sequences, extending the methodology should be based on certain assumptions and conventions and these include the following:

1. *Accounting for Chain End Entities.* These are assumed to be homogeneously distributed and can be postassigned to the specific chain, eliminating the need to model multiple populations and solve any extra model equations.

2. *Chain Orientation Convention.* The propagating radical chains are assumed to grow from left to right, i.e., always place the radical center at the rightmost end of the code. Dead polymer chains are assumed to inherit the orientation of a terminating chain radical by disproportionation while there will be a code flip in the case of termination by combination as discussed in details in the following sections.

3. *Elimination of Duplicated and Unused Codes.* The issues of duplicated and unused codes, resulting from differing chain lengths and higher arithmetic bases, respectively, must be eliminated. As for code duplication, some chains can start (on the left side) with a "0", making it possible to have two chains of differing lengths but of identical codes. For example, a chain of length 6 but having the sequence 110110 has the identical decimal equivalent, $d = 54$, as the chain of length 7 which has the sequence 0110110.

For unused codes, the issue arises at higher arithmetic bases and gaps of totally wasted codes will separate the sequence distribution at different polymer chain lengths, leading to an inefficient use of the total available codes and eventually to incontigous graphical representation. The convention used by Debling and Teymour[1] took care only of code duplication and not of the unused codes. It basically depended on adding a chain length bit of a "1" to the left-hand side of the code so that the two sequences of the previous example become 1110110 and 10110110, respectively. Hence, the precise monomeric sequence of any polymeric isomer of any length n is provided by a new modified decimal equivalent, S

$$S = d + 2^n \tag{1}$$

and

$$d = \sum_{i=1}^{n} b^{i-1} \nu_i \tag{2}$$

where n is the length of the sequence, b is the base of arithmetic, i is the position along the sequence (starting from the rightmost bit), and ν_i is the digit value ("0" or "1") at position i. A more general convention that avoids both duplicate and unused codes of polymer chains at any arithmetic base and provides contiguous sequences coding is proposed in this work. This convention takes into consideration both monomer sequence, represented by the decimal equivalent, and all preceded chain lengths, and S becomes

$$S = d + \sum_{i=1}^{n} b^{i-1} \tag{3}$$

The digital encoding technique can be used to graphically represent two different types of distributions that were not previously possible at the level of distinguishing polymeric isomers. The first is the encoded sequence length distribution (SLD), and the second is the chain type distribution (CTD). The statistics of monomeric sequence distributions have long been used as measures of structural differences,[16] mostly because these are measurable to some degree by NMR techniques. Traditionally, NMR analysis was limited to triad and tetrad distributions, but recent developments in NMR equipment allow for the distinction of longer sequences up to heptads.[17,18]

Debling and Teymour[1] have demonstrated that digital encoding can be combined with sequence length calculations to obtain a graphical representation of SLD, which adds a lot of insight into the types of structural differences to be expected at different reactivity ratio combinations. However, the more powerful feature of the digital encoding technique is that it enables the distinction of entire polymeric chains as entities uniquely identified by their decimal equivalent codes. Because of this distinction, one is then able to utilize the information represented by the reaction mechanism to write balances that account for the generation and/or consumption of all chains belonging to a specific code or alternately a specific chain type, hence the name "chain type distribution" (CTD). This approach of deriving population balances is routinely used in polymer reaction

CDV

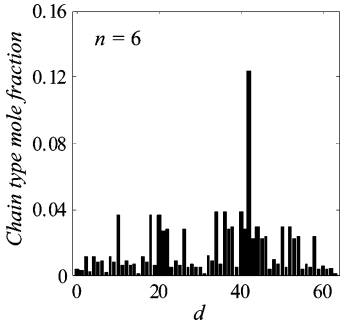

Figure 1. Chain type distribution (CTD) for chain length of 6 in a steady-state CSTR at 80 °C and for termination by disproportionation. $r_0 = 0.523$, $r_1 = 0.46$, $f_0 = 0.531$, and $Dp_n = 160$.

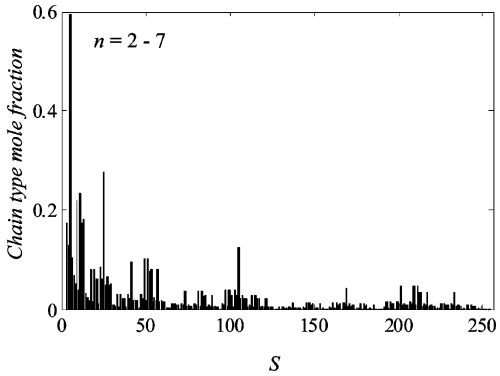

Figure 2. Chain type distribution (CTD) for consecutive chain lengths of 2−7 in a steady-state CSTR at 80 °C and for termination by disproportionation. $r_0 = 0.523$, $r_1 = 0.46$, $f_0 = 0.531$, and $Dp_n = 160$.

engineering to distinguish populations of chains having different chain lengths, number of pendant groups, or other features of the polymer chain. It is extended here to the distinction of populations by their digital code, which effectively encapsulates all the information about the polymer chain architecture in a unique descriptive manner. Details of the derivation of these population balances are presented in the following section.

The reader will notice that the CTD up to chain length 7 is generated and of chain length 6 is chosen throughout the text as a representative chain length. While this is done for the sake of computational simplicity, it is by no means restrictive to the predictive abilities of the model. CTDs up to chain length of 24 have been so far generated. The premise of this approach is that the mechanism that generates the polymer chain structure is the same at any chain length, thus the emergence of patterns in the CTD is expected. As a matter of fact, under certain conditions, the examination of short chain length CTDs can be much more revealing than those for long chains, since these deviate the most from the often used "long chain" approximation.

Patten recognition techniques and code compression methods can be used to arbitrarily extend the computations of a limited number of chains for any chain length. In regard of the pattern recognition and based on self-similarity concepts of fractal geometry, we managed to discover and decode the fractal in CTD and prove that CTD of short chain length is similar to that of longer chain length but at a different scale. Currently, the detailed work on this subject is under preparation to be submitted for publication.

Mathematical Model Development

We consider a free radical copolymerization process obeying the terminal model, and the mechanism is summarized in Table 1. The effect of each reaction step on the digital code of a specific chain type is first discussed to explain the rationale used in developing the population balance equations; then, these

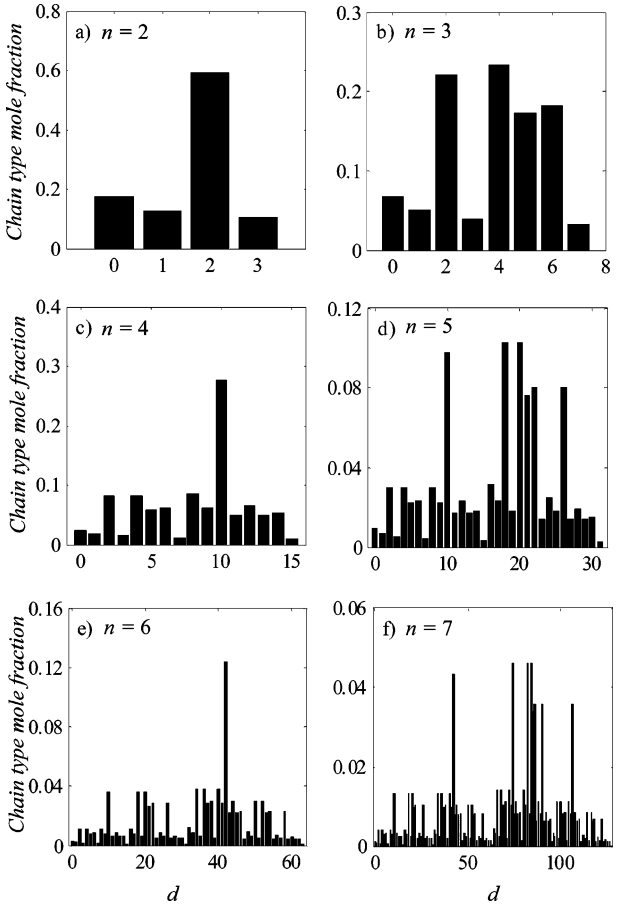

Figure 3. Chain type distribution (CTD) in a steady-state CSTR at 80 °C and for termination by disproportionation. $r_0 = 0.523$, $r_1 = 0.46$, $f_0 = 0.531$, and $Dp_n = 160$. (a−f): chain length, $n = 2-7$, respectively.

Table 1. Free Radical Copolymerization Mechanism/Terminal Model

Initiation	
Initiator	$I \xrightarrow{k_d} 2R_{0,0}$
Chain initiation	$R_{0,0} + M_j \xrightarrow{k_{pj}} R_{1,j}$
Propagation	$R_{n,d} + M_j \xrightarrow{k_{pij}} R_{n+1,Z}$
	where,
	$Z = \begin{cases} 2d, & \text{for } j = 0, \\ 2d+1, & \text{for } j = 1. \end{cases}$
Chain Transfer	
to monomer	$R_{n,d} + M_j \xrightarrow{k_{ctMij}} P_{n,d} + R_{1,j}$
to solvent	$R_{n,d} + S \xrightarrow{k_{ctSi}} P_{n,d} + R_{0,0}$
Chain Termination	
by disproportionation	$R_{n,d} + R_{m,e} \xrightarrow{k_{tdij}} P_{n,d} + P_{m,e}$
by combination	$R_{n,d} + R_{m,e} \xrightarrow{k_{tcij}} P_{n+m,g}$
	where,
	$g = 2^m d + \bar{e}$,
	$\bar{e}$ is the mirror image of e

are combined to obtain the model equations. The model presented in this article is developed for an isothermal continuous stirred tank reactor (CSTR), and the model equations are developed for a dynamic system, but their solution is restricted to steady-state operation. The effect of compositional drift on digital codes during CSTR transients or in batch operation was considered, and chain distributions for the semibatch system operating under composition control policies were analyzed in previous work.[19,20]

Initiation is the first necessary step in producing free radicals and in assigning codes. The homolytic decomposition of an initiator is considered to form a pair of primary radicals $R_{0,0}$ where $R_{n,d}$ is the radical of chain length, n, and a binary code, d. These primary radicals add to the two monomer molecules and produce the chain initiating species, $R_{1,0}$ and $R_{1,1}$, i.e., radicals of chain length 1 and ending with either code "0" or "1" depending on the identity of the added monomer.

Monomers, M_0 and M_1, can each add either to a propagating chain ending with M_0 or to a one ending with M_1. When a new monomer unit is inserted to the right of an existing binary string, a shift by one bit to the left will occur. This is mathematically equivalent to multiplying each bit by a factor of 2 and then adding the proper code, "0" or "1", for the acquired monomer unit. By doing so, the identity of the propagating radicals is revealed by whether its code is odd or even. An even code indicates a radical center involving M_0, and an odd code indicates M_1.

Chain transfer reactions involve the transfer of the free radical center from a growing chain to M_0, M_1, and solvent molecules. This produces dead polymers bearing the same code as their parent radical, while the new formed radicals bear codes according to the convention used in the initiation step with no distinction between the initiator fragment and the solvent molecule. Chain transfer to polymer was not considered as we are concerned with linear copolymers at this stage, though the extension of the technique to branched copolymers is considered for future work.

Termination reactions involve the formation of dead polymer chains for which the binary code is determined by the codes of the terminating radicals. Termination by disproportionation simply terminates the chain with no change in the binary sequence code inherited from the parent radical. Termination by combination is a little more complicated as it is the result of coupling two live radicals. Because of the convention of assigning the radical center to the right-hand side of the growing chain, "flipping" of the binary sequence of one of the radicals, the radical considered last, must be involved to translate the code to its mirror image. For each binary sequence there are a number of possible combinations of chain fragments that result in the same polymer chain size and binary code. Therefore, the model equation must consider all possible combinations of sequence codes d and e that form a code of sequence g.

For the principal mechanism shown in Table 1, the rates of change equations for all species are derived and the moments are defined according to the method of moments.[21] The moment equations combined with the mass balance equations of all species in the reaction system form the fundamental equations of the model.

Mass Balance Equations for Nonpolymer Species

- Initiator:

$$\frac{dC_I}{dt} = \frac{q}{V}(C_{Iin} - C_I) - fk_dC_I \tag{4}$$

where C_I is the initiator concentration (mol/L), q is the volumetric flow rate (L/s), V is the volume (l), and f is the initiator efficiency.

- Monomer j:

$$\frac{dC_{Mj}}{dt} = \frac{q}{V}(C_{Mjin} - C_{Mj}) - k_{pj}C_{R_{0,0}}C_{Mj} - C_{Mj}\sum_{i=0}^{1}(k_{pij} + k_{ctMij})\mu_{0,i} \tag{5}$$

- Solvent:

$$\frac{dC_S}{dt} = \frac{q}{V}(C_{Sin} - C_S) - C_S\sum_{i=0}^{1}k_{ctSi}\mu_{0,i} \tag{6}$$

- Primary radical:

$$\frac{dC_{R_{0,0}}}{dt} = 2fk_dC_I + C_S\sum_{i=0}^{1}k_{ctSi}\mu_{0,i} - C_{R_{0,0}}\sum_{j=0}^{1}k_{pj}C_{Mj} - C_{R_{0,0}}\sum_{i=0}^{1}(k_{tdpri} + k_{tcpri})\mu_{0,i} \tag{7}$$

- Radical of length one:

$$\frac{dC_{R_{1,j}}}{dt} = k_{pj}C_{R_{0,0}}C_{Mj} + C_{Mj}\sum_{i=0}^{1}k_{ctMij}\mu_{0,i} - C_{R_{1,j}}\sum_{i=0}^{1}(k_{pji} + k_{ctMji})C_{Mi} - k_{ctSj}C_{R1,j}C_S - C_{R1,j}\sum_{i=0}^{1}(k_{tdji} + k_{tcji})\mu_{0,i} \tag{8}$$

Mass Balance Equations for Polymer Species

- Growing polymer chains with end group i:

$$\frac{dC_{R_{n,d}}}{dt} = k_{pi}C_{R_{0,0}}C_{Mi} + \sum_{j=0}^{1}k_{ctMji}\mu_{0,j}C_{Mi} + \sum_{j=0}^{1}k_{pji}C_{Rn-1,X}C_{Mi} - C_{Rn,d}\sum_{j=0}^{1}(k_{pij} + k_{ctMij})C_{Mj} - k_{ctSi}C_{R_{n,d}}C_S - C_{R_{n,d}}\sum_{j=0}^{1}(k_{tdij} + k_{tcij})\mu_{0,j} \tag{9}$$

where

$$X = \begin{cases} d/2, & \text{for } i = 0 \\ (d-1)/2, & \text{for } i = 1 \end{cases}$$

Applying the quasi-steady-state approximation (QSSA) to radical balances, eqs 7 and 8 yield the following expressions:

$$C_{R_{0,0}} = \frac{2fk_dC_I + C_S\sum_{i=0}^{1}k_{ctSi}\mu_{0,i}}{\sum_{j=0}^{1}k_{pj}C_{Mj} + \sum_{i=0}^{1}(k_{tdpri} + k_{tcpri})\mu_{0,i}} \quad (10)$$

$$C_{R_{1,0}} = \frac{k_{p0}C_{R_{0,0}}C_{M0} + C_{M0}\sum_{i=0}^{1}k_{ctMi0}\mu_{0,i}}{\sum_{i=0}^{1}(k_{p0i} + k_{ctM0i})C_{Mi} + k_{ctS0}C_S + \sum_{i=0}^{1}(k_{td0i} + k_{tc0i})\mu_{0,i}} \quad (11)$$

$$C_{R_{1,1}} = \frac{k_{p1}C_{R_{0,0}}C_{M1} + C_{M1}\sum_{i=0}^{1}k_{ctMi1}\mu_{0,i}}{\sum_{i=0}^{1}(k_{p1i} + k_{ctM1i})C_{Mi} + k_{ctS1}C_S + \sum_{i=0}^{1}(k_{td1i} + k_{tc1i})\mu_{0,i}} \quad (12)$$

For any growing polymer chain of length $n \geq 2$, there are four cases to be considered as discussed in eq 9, depending on the type of both the propagating radical and the monomer added to it. These four types of propagating radicals will be digitally identified by the last two rightmost bits in the chain binary code which will be ∼00•, ∼01•, ∼10•, and ∼11•, which are expressed as follows after the application of QSSA:

1. Growing polymer chains ending with ∼00•:

$$C_{R_{n,d}} = \frac{k_{p00}R_{n-1,d/2}C_{M0}}{\sum_{j=0}^{1}(k_{p0j} + k_{ctM0j})C_{Mj} + k_{ctS0}C_S + \sum_{j=0}^{1}(k_{td0j} + k_{tc0j})\mu_{0,j}} \quad (13)$$

2. Growing polymer chains ending with ∼01•:

$$C_{R_{n,d}} = \frac{k_{p01}R_{n-1,(d-1)/2}C_{M1}}{\sum_{j=0}^{1}(k_{p1j} + k_{ctM1j})C_{Mj} + k_{ctS1}C_S + \sum_{j=0}^{1}(k_{td1j} + k_{tc1j})\mu_{0,j}} \quad (14)$$

3. Growing polymer chains ending with ∼10•:

$$C_{R_{n,d}} = \frac{k_{p10}R_{n-1,d/2}C_{M0}}{\sum_{j=0}^{1}(k_{p0j} + k_{ctM0j})C_{Mj} + k_{ctS0}C_S + \sum_{j=0}^{1}(k_{td0j} + k_{tc0j})\mu_{0,j}} \quad (15)$$

4. Growing polymer chains ending with ∼11•:

$$C_{R_{n,d}} = \frac{k_{p11}R_{n-1,(d-1)/2}C_{M1}}{\sum_{j=0}^{1}(k_{p1j} + k_{ctM1j})C_{Mj} + k_{ctS1}C_S + \sum_{j=0}^{1}(k_{td1j} + k_{tc1j})\mu_{0,j}} \quad (16)$$

• Dead polymer chains:

$$\frac{dC_{P_{n,g}}}{dt} = -\frac{q}{V}C_{P_{n,g}} + \sum_{i=0}^{1}\sum_{j=0}^{1}k_{ctMij}C_{Rn,g}C_{Mj} + C_S\sum_{i=0}^{1}k_{ctSi}C_{R_{n,g}} + \sum_{i=0}^{1}\sum_{j=0}^{1}k_{tdij}C_{R_{n,g}}\mu_{0,j} + \frac{1}{2}\sum_{i=0}^{1}\sum_{j=0}^{1}\sum_{m=1}^{n-1}k_{tcij}C_{Rm,d}C_{Rn-m,e} \quad (17)$$

where $g = 2^j d + \bar{e}$ and $\bar{e}$ is the mirror image of e.

Moment Equations. The moment equations for all polymer species are derived using the moments defined in Table 2. By calculating these moments, the number- and weight-average degree of polymerization can be predicted. Note that the QSSA applies, $d\mu/dt = 0$, and the live moments are directly deduced from their rate of change equations.

• Growing polymer chains, zeroth moment; $\mu_{0,j}$and μ_0:

$$\mu_{0,0} = \frac{\mu_0}{1 + \frac{C_{M1}}{C_{M0}}\left(\frac{k_{p01} + k_{ctM01}}{k_{p10} + k_{ctM10}}\right) + \frac{C_S}{C_{M0}}\left(\frac{k_{ctS0}}{k_{p10} + k_{ctM10}}\right)} \quad (18)$$

$$\mu_{0,1} = \frac{\mu_0}{1 + \frac{C_{M0}}{C_{M1}}\left(\frac{k_{p10} + k_{ctM10}}{k_{p01} + k_{ctM01}}\right) + \frac{C_S}{C_{M1}}\left(\frac{k_{ctS1}}{k_{p01} + k_{ctM01}}\right)} \quad (19)$$

$$\mu_0 = \sum_{j=0}^{1}\mu_{0,j} \quad (20)$$

• Growing polymer chains, first moment; $\mu_{1,j}$and μ_1:

$$\mu_{1,0} = \frac{k_{p0}C_{R_{0,0}}C_{M0} + C_{M0}\sum_{i=0}^{1}(k_{pi0} + k_{ctMi0})\mu_{0,i}}{\sum_{i=0}^{1}k_{ctM0i}C_{Mi} + k_{ctS0}C_S + \sum_{i=0}^{1}(k_{td0i} + k_{tc0i})\mu_{0,i}} \quad (21)$$

$$\mu_{1,1} = \frac{k_{p1}C_{R_{0,0}}C_{M1} + C_{M1}\sum_{i=0}^{1}(k_{pi1} + k_{ctMi1})\mu_{0,i}}{\sum_{i=0}^{1}k_{ctM1i}C_{Mi} + k_{ctS1}C_S + \sum_{i=0}^{1}(k_{td1i} + k_{tc1i})\mu_{0,i}} \quad (22)$$

$$\mu_1 = \sum_{j=0}^{1}\mu_{1,j} \quad (23)$$

• Growing polymer chains, second moment; $\mu_{2,j}$ and μ_2:

$$\mu_{2,0} = \frac{k_{p0}C_{R_{0,0}}C_{M0} + C_{M0}\sum_{i=0}^{1}(k_{pi0} + k_{ctMi0})\mu_{0,i} + C_{M0}\sum_{i=0}^{1}k_{pi0}2\mu_{1,i}}{\sum_{i=0}^{1}k_{ctM0i}C_{Mi} + k_{ctS0}C_S + \sum_{i=0}^{1}(k_{td0i} + k_{tc0i})\mu_{0,i}} \quad (24)$$

$$\mu_{2,1} = \frac{k_{p1}C_{R_{0,0}}C_{M1} + C_{M1}\sum_{i=0}^{1}(k_{pi1} + k_{ctMi1})\mu_{0,i} + C_{M1}\sum_{i=0}^{1}k_{pi1}2\mu_{1,i}}{\sum_{i=0}^{1}k_{ctM1i}C_{Mi} + k_{ctS1}C_S + \sum_{i=0}^{1}(k_{td1i} + k_{tc1i})\mu_{0,i}} \quad (25)$$

$$\mu_2 = \sum_{j=0}^{1}\mu_{2,j} \quad (26)$$

Table 2. Polymer Chain and Moments Definitions

R_n	a growing polymer chain with n monomer units
P_n	a dead polymer chain with n monomer units
μ_f	growing polymer moments $\mu_f = \Sigma_{n=1}^{\infty} n^f R_n$ and $\mu_f = \Sigma_{j=0}^{1} \mu_{f,j}$, where $\mu_{f,j}$ is the fth moment for growing polymer chains ending with "j" code
λ_f	dead polymer moments $\lambda_f = \Sigma_{n=1}^{\infty} n^f P_n$ and $\lambda_f = \Sigma_{j=0}^{\infty} \lambda_{f,j}$, where $\lambda_{f,j}$ is the fth moment for dead polymer chains ending with "j" code

• Dead polymer zeroth, first, and second moments, λ_0, λ_1, and λ_2, respectively

$$\frac{d\lambda_0}{dt} = -\frac{q}{V}\lambda_0 + \sum_{i=0}^{1}\sum_{j=0}^{1} k_{ctMij}\mu_{0,i}C_{Mj} + C_S\sum_{i=0}^{1} k_{ctSi}\mu_{0,i} + \sum_{i=0}^{1}\sum_{j=0}^{1}(k_{tdij} + 1/2\, k_{tcij})\mu_{0,i}\mu_{0,j} \quad (27)$$

$$\frac{d\lambda_1}{dt} = -\frac{q}{V}\lambda_1 + \sum_{i=0}^{1}\sum_{j=0}^{1} k_{ctMij}\mu_{1,i}C_{Mj} + C_S\sum_{i=0}^{1} k_{ctSi}\mu_{1,i} + \sum_{i=0}^{1}\sum_{j=0}^{1}(k_{tdij} + k_{tcij})\mu_{0,i}\mu_{1,j} \quad (28)$$

$$\frac{d\lambda_2}{dt} = -\frac{q}{V}\lambda_2 + \sum_{i=0}^{1}\sum_{j=0}^{1} k_{ctMij}\mu_{2,i}C_{Mj} + C_S\sum_{i=0}^{1} k_{ctSi}\mu_{2,i} + \sum_{i=0}^{1}\sum_{j=0}^{1} k_{tdij}\mu_{0,i}\mu_{2,j} + \sum_{i=0}^{1}\sum_{j=0}^{1} k_{tcij}(\mu_{0,i}\mu_{2,j} + \mu_{1,i}\mu_{1,j}) \quad (29)$$

Solution of Model Equations. Beginning at the initial time with the initial conditions, the dynamic model equations, eqs 4−6, 10−12, and 13−20, are solved simultaneously by Runge−Kutta formula which is built in MATLAB 6.5 release 13 as ode45 algorithm. In computing a variable at time (t), ode45 needs only the solution at the immediately preceding time point at ($t - 1$).

When a steady-state solution is required, the steady-state forms of the nonpolymer species mass balance equations, eqs 4−7, and the zeroth moment equations, eqs 18−20, are solved simultaneously by Newton−Raphson method, and their solution is substituted in eqs 11−17 to solve explicitly for radical and dead polymer chain type concentrations.

Chain Type Distribution (CTD): A New Distribution. The notion of chain type distribution is defined as the number or mole fraction distribution, of all chain types including the polymeric isomers for every chain length, where each chain type is represented by a digital code that reflects its architectural features.

On the basis of the mathematical model equations, Figure 1 illustrates CTD for a copolymerization reaction obeying the terminal model in a steady-state CSTR at 80 °C and a steady-state comonomer composition of $f_0 = 0.531$ when termination is by disproportionation. Table 3 shows the kinetic parameters used in simulations. The decomposition rate constant is for AIBN as an initiator, homopropagation rate constants are for styrene and methyl methacrylate as monomers and are considered to be independent of chain length, thus $k_{pj} = k_{pij}$ and (j = 0, 1), cross-propagation rate constants are calculated according to considered reactivity ratios where $k_{ij} = k_{ii}/r_i$, while $r_0 = 0.523$ and $r_1 = 0.46$ are the optimum reactivity ratio values for styrene/methyl methacrylate system according to Fukuda et al.[23] Differentiation between termination modes of disproportionation and combination is considered, and for this purpose termination rate constants are considered to be equal and chosen arbitrary to equal that of styrene, unless mentioned otherwise when complications of termination mechanisms are investigated.

Table 3. Kinetic Parameters Used in Simulations/Terminal Model

kinetic parameters	
k_d (s^{-1})	$1.58E + 15 \exp(-30800/RT)$[ref 22]
	R (cal/(mol K)), T (K)
k_{p00} (L/(mol s))	$3.16E + 7 \exp(-7761.80^{\text{ref 24}}/RT)$
k_{p11}(L/(mol s))	$2.02E + 6 \exp(-5339.58^{\text{ref 25}}/RT)$
k_{p0} (L/(mol s))	k_{p00} (assumption)
k_{p1}(L/(mol s))	k_{p11} (assumption)
k_{ctMij}, k_{ctSi} (L/(mol s))	0
k_{tdpri}, k_{tcpri} (L/(mol s))	$8.6E + 8 \exp(-1677.03/RT)$
k_{tdij}, k_{tcij} (L/(mol s))	$8.6E + 8 \exp(-1677.03/RT)$
r_0	$k_{p00}/k_{p01} = 0.523$[ref 23]
r_1	$k_{p11}/k_{p10} = 0.46$[ref 23]

Figure 1 represents the histogram of chain type mole fraction in terms of the decimal equivalent of the binary code (d) for a chain length of 6. Each bar in the histogram reflects a chain type ranging from a code of all zero digits 000000 at $d = 0$ to a code of all ones 111111 at $d = 63$. That includes 64 chain types for a chain length of 6, i.e., the number of chain types for a binary copolymerization system $= 2^n$, where n is the chain length. The histogram has two distinctive groups depending on the identity of the monomer directly attached to the chain end entities (e.g., initiator fragment), assuming they are indistinguishable in this case. The first group has chains starting always with M_0 and ending with M_0 and M_1 interchangeably, and their codes range from $d = 0$ to $d = 31$. The second group has chains starting always with M_1 and ending with M_0 and M_1 interchangeably, and their codes range from $d = 32$ to $d = 63$. This distinction of groups is important in analyzing similarities and in detection of patterns in CTD.

A second feature of CTD is the dominance of certain chains over others; these chain types are expected to influence the physical and mechanical properties of a polymer. Therefore, when the chain type distribution is altered, dominant chains are mostly responsible to differences in the observed performance properties of the polymer. In this example, chain type 101010 at $d = 42$ is strongly dominant, followed by chains of sequences 100010, 100100, and 101000 at $d = 34$, 36, and 40, respectively.

A modified decimal equivalent (S) is used to represent a contiguous CTD for propagating chain lengths, avoiding both duplicate and unused codes of polymer chains at any arithmetic base. Consequently, it is possible to alter the representation of CTD in terms of S as shown in Figure 2 for chain lengths of 2−7. For the sake of getting used to both decimal equivalents, (d) is used to represent CTD of one chain length and (S) is used to represent CTD for consecutive chain lengths. Figure 2 can be analyzed in further details if we zoom in and allow the distributions of every chain length to be plotted separately. Figure 3a−f illustrates these distributions for chain lengths 2−7 and in terms of decimal equivalent (d). The decimal equivalent d serves as a measure of how chain type numbers increase exponentially with increasing chain length. At chain length 2 there are 4 chain types, and at chain length 7 there are 128 chain types. This increase in chain length means an exponential increase in the model equations needed to be solved. CTD simulation time takes less than a second for a chain length of 2 and 4 min for a chain length of 20. Beyond that length the

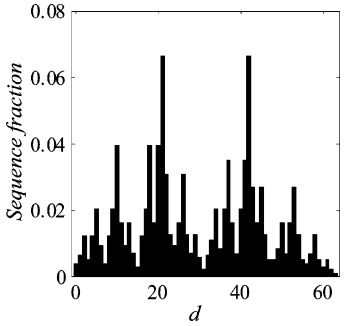

Figure 4. Sequence length distribution (SLD) for sequence length of 6. $r_0 = 0.523$, $r_1 = 0.46$, $f_0 = 0.531$, and $Dp_n = 160$.

computer's memory becomes a limitation. Note that MATLAB simulations are run in Pentium 4 CPU 2.40 GHz, 512 MB of RAM PC. Nevertheless, these current computational limitations are not of much concern because by the digital encoding technique, it is possible to extract more precise information about the copolymerization system based on the analysis of short chains. Our argument is supported by CTD results shown in Figures 2 and 3a−f, in which the mole fractions and polymer chain types are substantially different for shorter chains and by this allowing the possibility of measurement using sequence-sensitive analytical techniques.[17,18]

There are other two features of CTD that are illustrated in Figure 3a−f: the switch of CTD pattern depending if the chain length is odd or even, and the similarity between CTD at any odd chain length or at any even chain length. A direct consequence of these features is the dominance of certain sequences that appear at relatively same regions of CTD. Remember that the chain length is increasing, and on the basis of observed similarity, one can deduce that there might be a relationship between the dominant chains of relatively same regions in CTD at different chain lengths. These similarities, if proven to have imbedded patterns, can support the prediction of CTD for any chain length from short chains, and the argument that short chains are representative of the copolymerization system can be verified.

Encoded Sequence Length Distribution (SLD) vs Chain Type Distribution (CTD). Encoded SLD was presented earlier by Debling and Teymour,[1] while CTD is completely developed in this work and generated from the mathematical model equations as already shown in Figures 1, 2, and 3a−f.

Basically, SLD is generated from the probabilistic calculations which are strictly based on the "long-chain approximation" (LCA). This assumption states that polymer chains are sufficiently long that SLD will only be affected by propagation reactions where initiation and terminations reactions can be neglected. The restriction to long chains is mainly because statistical derivations implicitly assumes QSSA and short chains may exhibit composition transients before the steady-state composition is reached due to monomers not initiated at the quasi-steady-state ratio R_0/R_1.[16,26]

By applying the digital encoding technique, the probability of occurrence of any specific sequence of monomers, say 1011001, is calculated as the combined probability that a propagating radical terminated in 1 will add 0, then 1, then 1, and so on. The statistics generated for all types of sequences of a particular length are then studied as these can be compared to measurements by NMR.

Figure 4 depicts SLD under same kinetic and process conditions as in Table 3 and is represented in terms of the decimal equivalent (*d*). The qualitative and quantitative differences are very clear between SLD and CTD results of Figure 4 and Figure 1, respectively. SLD represents the distribution of

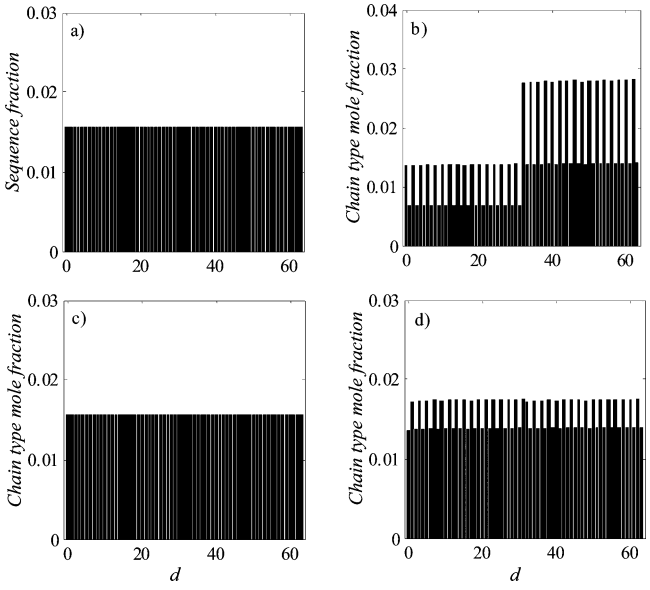

Figure 5. (a) SLD for sequence length of 6, $r_0 = r_1 = 1.0$, $f_0 = 0.5$, and kinetic parameters as in Table 3. (b−d) CTD in a steady-state CSTR at 80 °C and for chain length of 6 and termination by disproportionation: (b) $r_0 = r_1 = 1.0$, $f_0 = 0.5$ and kinetic parameters as in Table 3. (c) $r_0 = r_1 = 1.0$, $f_0 = 0.5$, and $k_{pj} = k_{pij} = 3.16E + 10 \exp(-7761.8/RT)$. (d) Normalized CTD of case (b).

sequences of length 6 in long copolymer chains while CTD represents the distribution of copolymer chains of length 6. Each of these distributions displays the microstructure heterogeneity differently. Dissimilarity in dominating sequences and chains is one example. Figure 4 demonstrates that SLD dominant sequences are 010101 and 101010 at $d = 21$ and 42, respectively, followed by sequences 001010, 010010, and 010100 at $d = 10$, 18, and 20, respectively, while Figure 1 for CTD shows that chain 101010 at $d = 42$ is strongly dominant followed by chains 100010, 100100, and 101000 at $d = 34$, 36, and 40, respectively.

As a second example, what might be thought of as a truly random copolymer with respect to sequences is not so with respect to chain types. Figure 5a,b clarifies this point, where for SLD all sequences have equal probabilities but CTD chain distribution splits in 4 different groups depending on the identity of monomer attached to chain end entities. Note that both calculations are done under the same conditions as in Table 3 but for $r_0 = r_1 = 1.0$. CTD becomes truly random as that in Figure 5c if and only if chain initiation (k_{pj}) and propagation (k_{pij}) rate constants are all equal and $f_j = 0.5$. This finding is in contrast with that of Flory's based on sequences; "$r_1 r_2 = 1$ ⋯ for $r_1 = 1$ represents the trivial case in which $k_{p11} = k_{p12}$ and $k_{p22} = k_{p21}$, i.e., that in which the two monomers are equally reactive with each radical. (The reactivities of the two radicals might differ however; i.e., k_{p11} need not equal k_{p22}.[27]) Subscripts of "1" and "2" in Flory's representation of monomers 1 and 2 are equivalent to the digital encoding technique representation of "0" and "1", respectively.

One might argue that the differences between SLD and CTD of Figure 5a,b, respectively, is a consequence of the chain orientation convention and that if CTD is normalized; i.e., if concentrations of each chain type and its mirror image are averaged, then the resemblance between SLD and CTD will be evident. Figure 5d is the normalized CTD of Figure 5b and is still distinctive from SLD. The main reason lies in accounting for unequal chain initiation and propagation rate constants that alters the distribution for short chains in CTD but has a negligible effect on sequences of long copolymer chains in SLD

that is affected by reactivity ratio rather than individual rate constants.

Results and Discussion

We consider a copolymerization reaction obeying the terminal model. Table 3 shows the kinetic parameters used in simulations. The following analysis includes the theoretical investigation of varying the reactivity ratios, the comonomer compositions, and when the growing polymer chain is either terminated by disproportionation or combination. Then, the digital encoding technique is applied to a case study of styrene/methyl methacrylate system in which a theoretical discrimination between terminal and penultimate models and differentiation between termination mechanisms are pursued. Finally, the complexity of the generated results is assessed by entropy calculations.

Effect of Reactivity Ratios. In classifying copolymerizations in terms of reactivity ratios, the reference must go to Figure 6, where the instantaneous copolymer composition with respect to M_0, F_0, is plotted vs comonomer composition, f_0, for the terminal model. Figure 7a−f corresponds to CTD of various reactivity ratio combinations that are illustrated in Figure 6, at steady-state comonomer composition, $f_0 = 0.5$, when termination is solely by disproportionation and for $r_0 = r_1 = 0.1$, 0.5, 1.0, 2.0 and the ideal cases $r_0 = 0.1$, $r_1 = 10.0$ and $r_0 = 0.5$, $r_1 = 2.0$, respectively. Figure 7a−d shows the effect of increasing the reactivity ratios when these are kept equal. At $r_0 = r_1 = 0.1$, Figure 7a shows that cross-propagation is preferred to homopropagation, and the polymer tends to have an alternating architecture as evidenced by the two dominant alternating sequences 010101 and 101010 at $d = 21$ and 42, with stronger preference to 101010 over 010101. As discussed earlier, this is not a consequence of the chain orientation convention but because of considering unequal chain initiation and propagation rate constants. As the reactivity ratios increase, the alternating sequence 101010 is still dominant but with other chain types catching up until $r_0 = r_1 = 1.0$ where 4 different chain type groups are formed and each consists of 16 distinctive chain types, as shown in Figure 7c. A further increase of the reactivity ratios induces the preference of homopropagation to cross-propagation, resulting in the dominance of blockiness but shared with partially blocked copolymers as in Figure 7d. The treatment is extended to the ideal case, $r_0 r_1 = 1$, which allows for a difference between comonomer and copolymer compositions as $r_0 \neq 1$. Figure 7e shows that the dominant sequences are either 011111 at $d = 31$ or 111111 at $d = 63$ for $r_0 = 0.1$ and $r_1 = 10.0$. This means that blockiness is preferred, and it is difficult to produce copolymers containing considerable amounts of the two monomers unless when r_0 and r_1 do not differ much as shown in Figure 7f for $r_0 = 0.5$ and $r_1 = 2.0$.

Effect of Comonomer Composition. Figure 8a−c demonstrates CTD for M_0:M_1 wt % in feed of 35:65, 50:50, and 77:23, with steady-state comonomer composition $f_0 = 0.3$, 0.5, and 0.8, respectively. When the feed is richer in M_1, Figure 8a shows that the system is richer in chains initiated with M_1, and thus the second region of CTD with $d = 32-63$ is populated compared to the first region that represents chains initiated with M_0. As M_0 wt % in feed increases, more balance in CTD can be seen as in Figure 8b, with the dominance of any chain type dependent on the kinetic parameters. Further increase of M_0 causes the first region with $d = 0-31$ to become more populated. These investigated cases are for copolymerizations with comonomer composition different than that of copolymer. However, azeotropic copolymerization, at which comonomer and copolymer compositions are equal, are commercially desirable because a copolymer with as narrow a distribution of compositions can be obtained with the desired polymer properties that are dependent on copolymer composition.[28] But does the same azeotropic composition necessarily ensure the same microstructure which can also have a drastic effect on the polymer properties? Multiple combinations of reactivity ratios can lead to the same azeotropic composition, as seen for example by Figure 9a. Figure 9b−d shows the structure of this same azeotrope at composition $F_0 = f_0 = 0.531$ but for three different reactivity ratio combinations, $(r_0,r_1) = (0.38, 0.3)$, (0.523, 0.46), and (0.735, 0.7), respectively. It is obvious that CTD results are distinctively different, just confirming that the same azeo-

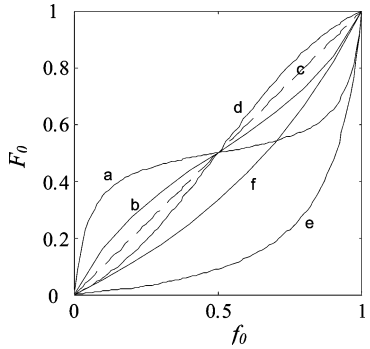

Figure 6. Copolymer composition with respect to monomer of code "0" vs comonomer composition for terminal model. (a) $r_0 = r_1 = 0.1$, (b) $r_0 = r_1 = 0.5$, (c) $r_0 = r_1 = 1.0$, (d) $r_0 = r_1 = 0.2$, (e) $r_0 = 0.1$ and $r_1 = 10.0$, (f) $r_0 = 0.2$ and $r_1 = 5.0$.

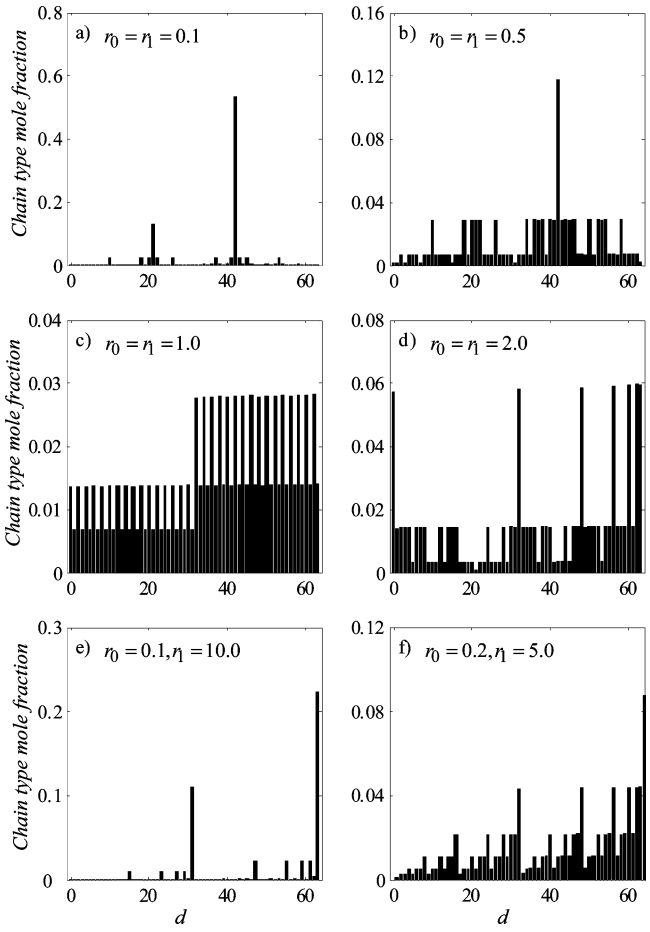

Figure 7. CTD for a chain length of 6 in a steady-state CSTR at 80 °C and for termination by disproportionation for $f_0 = 0.5$. (a) $r_0 = r_1 = 0.1$, (b) $r_0 = r_1 = 0.5$, (c) $r_0 = r_1 = 1.0$, (d) $r_0 = r_1 = 0.2$, (e) $r_0 = 0.1$ and $r_1 = 10.0$, (f) $r_0 = 0.2$ and $r_1 = 5.0$.

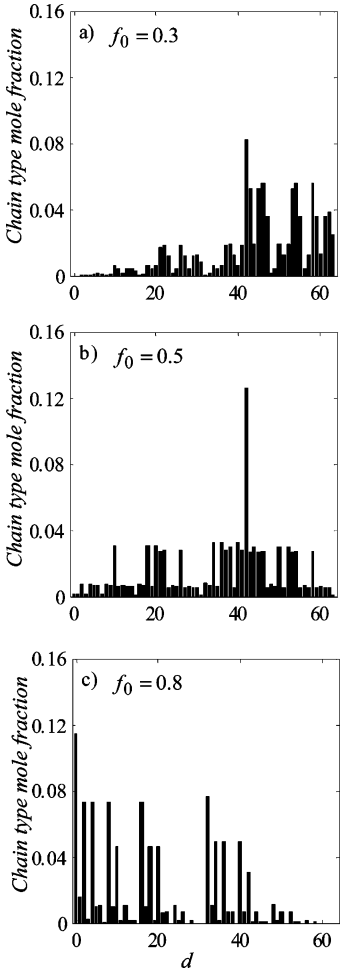

Figure 8. CTD for a chain length of 6 in a steady-state CSTR at 80 °C, for termination by disproportionation, $r_0 = 0.523$, and $r_1 = 0.46$. (a) M_0:M_1 wt % in feed = 35:65, $f_0 = 0.3$, and $Dp_n = 169$. (b) M_0:M_1 wt % in feed = 50:50, $f_0 = 0.5$, and $Dp_n = 160$. (c) M_0:M_1 wt % in feed = 77:23, $f_0 = 0.8$, and $Dp_n = 139$.

tropic composition does not imply the same microstructural properties of these azeotropes, and consequently can lead to vastly different polymer properties.

Effect of Termination Modes. So far free radical terminal model is examined when termination is considered totally by disproportionation. In the case of termination by combination, alternating and random cases at $r_0 = r_1 = 0.1$ and $r_0 = r_1 = 1.0$, respectively, are shown in Figure 10a,b. It demonstrates the appearance of additional sequences that were not dominant in CTD for termination by disproportionation. This is due to the more complicated fashion at which the live radicals are terminated causing the code of the last considered radical to flip and therefore result in a significant "shuffling" of the chain types. Note that CTD for termination by combination is normalized because the kinetic balance of each chain type considers the average of all possible combinations of radicals.

Nonetheless, in free radical copolymerizations, both termination modes are possible, and the identification of their contribution is a key to estimate termination rate constants. Figure 11a−c displays the influence of varying termination modes contribution on chain type distributions for $k_t = k_{td} + k_{tc} = 8.6E + 8 \exp(-1677.03/RT)$ and when termination by disproportionation to that by combination, k_{td}:k_{tc}, is 0.1:0.9, 0.5:0.5, and 0.9:0.1, respectively. Regardless of the change of termination mode contribution, a minimal difference is noticed as termination by disproportion results in much higher (4 orders of magnitude)

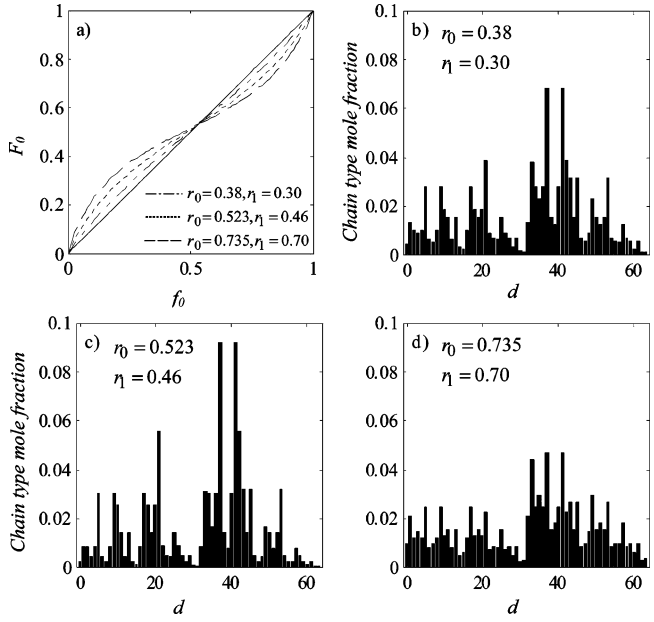

Figure 9. (a) Copolymer composition with respect to monomer of code "0" vs comonomer composition for terminal model. Solid line: (r_0,r_1) = (1.0, 1.0); dash−dotted line: (r_0,r_1) = (0.38, 0.30); dotted line: (r_0,r_1) = (0.523, 0.46); dashed line: (r_0,r_1) = (0.735, 0.70). (b−d) CTD for a chain length of 6 in a steady-state CSTR at 80 °C, for termination by disproportionation and for an azeotropic composition of $f_0 = F_0 = 0.531$: (b) $r_0 = 0.38$ and $r_1 = 0.30$, (c) $r_0 = 0.523$ and $r_1 = 0.46$, (d) $r_0 = 0.735$ and $r_1 = 0.70$.

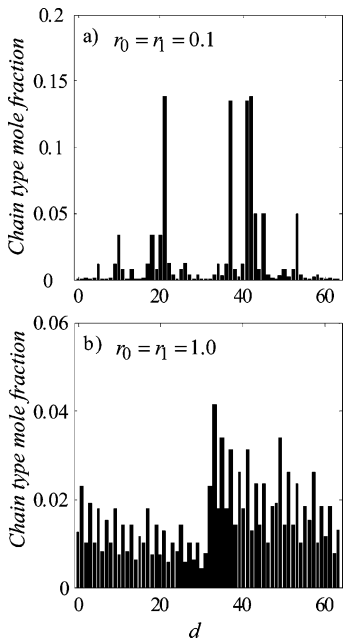

Figure 10. CTD for a chain length of 6 in a steady-state CSTR at 80 °C, for termination by combination, and for $f_0 = 0.5$. (a) $r_0 = r_1 = 0.1$, (b) $r_0 = r_1 = 1.0$.

polymer chain concentrations than in case of termination by combination, and as a result its effect dominates. Consequently, it is anticipated that unless k_t is orders of magnitude larger or/and termination mode contribution is vastly different, the effect of termination by combination will not be noticeable. This is demonstrated in Figure 12a−c in which $k_t = 8.6E + 10 \exp(-1677.03/RT)$, that is 2 orders of magnitude larger than the case of Figure 11a−c, for either 0.1:0.9, 0.5:0.5, or 0.9:0.1 of termination modes contribution. Termination by combination mode influence is more aggressive and could shuffle CTD as

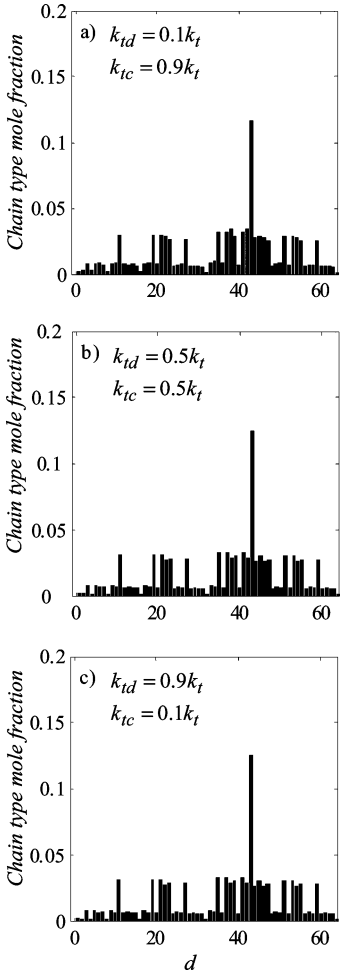

Figure 11. CTD for a chain length of 6 in a steady-state CSTR at 80 °C, for $k_t = 8.6E + 8\exp(-1677.03/RT) = k_{td} + k_{tc}$, and $f_0 = 0.5$. (a) $k_{td} = 0.1k_t$, $k_{tc} = 0.9k_t$, (b) $k_{td} = 0.5k_t$, $k_{tc} = 0.5k_t$, (c) $k_{td} = 0.9k_t$, $k_{tc} = 0.1k_t$.

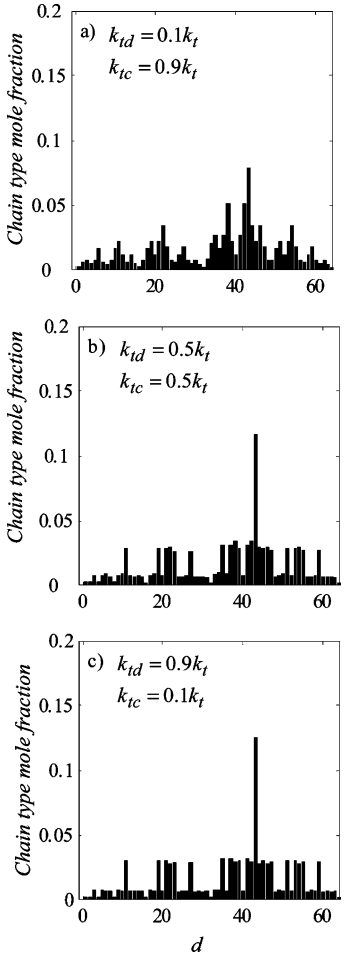

Figure 12. CTD for a chain length of 6 in a steady-state CSTR at 80 °C and for $k_t = 8.6E + 10\exp(-1677.03/RT) = k_{td} + k_{tc}$, and $f_0 = 0.5$. (a) $k_{td} = 0.1k_t$, $k_{tc} = 0.9k_t$, (b) $k_{td} = 0.5k_t$, $k_{tc} = 0.5k_t$, (c) $k_{td} = 0.9k_t$, $k_{tc} = 0.1k_t$.

shown in Figure 12a, but as its contribution decreases, its effect on CTD diminishes.

Case Study: Styrene/Methyl Methacrylate; Propagation Mechanism Discrimination. Considerable interest has been generated in the study of polymerization mechanisms over the years, especially after observing deviations from the terminal model. Numerous higher order copolymerization models have been suggested in order to explain these deviations.

Most of the investigations of copolymerization mechanisms involve the analysis of copolymer composition of initial copolymers formed, but it is often difficult to distinguish between the various models for copolymerization on the basis of their fit to the composition data alone.[17,18] Thus, Hill et al.[29] proposed that the distribution of monomer sequences in the copolymer, calculated on the basis of the statistical method, contains more information about the polymerization system than the copolymer composition. Hill et al. proposed that this information together with copolymer composition for copolymer prepared over the range of comonomer composition should discriminate between propagation models. In their work, styrene/maleic anhydride was investigated, and the kinetic parameters were calculated for four models: terminal, penultimate, complex participation, and complex dissociation. Although no triad measurements were made, the predictions of their models were sufficiently different to permit the use of such data to distinguish between the models investigated.

On the other hand, the distinction between models by sequence length information is not always possible, as in the case of styrene/methyl methacrylate. For this system both the terminal and penultimate models provide adequate fit for composition and sequence length data[30] as well as for the rate data.[31] Despite that fact, Fukuda et al.[23,32−34] investigated the styrene/methyl methacrylate system, and on the basis of rate data, they concluded that the terminal model fails, and as numerical values are concerned, their experimental data were well represented by the penultimate model. These results reflect the difficulty in distinguishing between different models with many parameters when relying on calculations of composition, sequence length, or rate.

Although, there is yet no analytical method to validate the digital encoding technique, it is proposed as appealing model discrimination tool because it provides chain type fraction distributions that are specific to distinguish polymer chains at same length down to their polymeric isomers, i.e., to an unprecedented level of specificity in microstructure. This capability is demonstrated, as follows, for styrene/methyl methacrylate copolymerization system to discriminate between terminal and penultimate models.

A digitally encoded kinetic terminal model for a free radical copolymerization system was formulated and discussed in detail in the mathematical model development section. The terminal model is a model in which the rate of reaction with a given type of monomer depends on the type of monomer bearing the

Table 4. Free Radical Copolymerization Mechanism/Penultimate Model

Initiation	
Initiator	$I \xrightarrow{k_d} 2R_{0,0}$
Chain initiation	$R_{0,0} + M_j \xrightarrow{k_{pj}} R_{1,j}$
Propagation	$R_{1,d} + M_j \xrightarrow{k_{pij}} R_{2,Z}$
	$R_{n,d} + M_k \xrightarrow{k_{pijk}} R_{n+1,Z}$
	where,
	$n=2,\ Z=\begin{cases}2d, & \text{for } j=0,\\ 2d+1, & \text{for } j=1.\end{cases}$,
	and
	$n>2,\ Z=\begin{cases}2d, & \text{for } k=0,\\ 2d+1, & \text{for } k=1.\end{cases}$
Chain Transfer	
to monomer	$R_{n,d} + M_k \xrightarrow{k_{ctMjk}} P_{n,d} + R_{1,k}$
to solvent	$R_{n,d} + S \xrightarrow{k_{ctSj}} P_{n,d} + R_{0,0}$
Chain Termination	
by disproportionation	$R_{n,d} + R_{m,e} \xrightarrow{k_{tdjk}} P_{n,d} + P_{m,e}$
by combination	$R_{n,d} + R_{m,e} \xrightarrow{k_{tcjk}} P_{n+m,g}$
	where,
	$g = 2^m d + \bar{e}$,
	$\bar{e}$ is the mirror image of e

radical. This implies four distinct propagation reactions and four types of growing radicals. For a chain of length $n = 2$ or greater, the produced radicals by propagation are digitally identified by the last two rightmost bits in the chain binary code which are ∼00•, ∼01•, ∼10•, ∼11•. On the other hand, the penultimate model is a model in which the identity of the last two monomer units of the chain determines the rate of propagation. Thus, for copolymerization of 2 monomers, eight distinct propagation reactions and eight types of growing radical with chain of length $n = 3$ or greater are digitally identified by the last three rightmost bits in the chain binary code which are ∼000•, ∼001•, ∼010•, ∼011•, ∼100•, ∼101•, ∼110•, ∼111•. The main modeling route accounts for longer terminal sequences, and this is translated mathematically into different growing radical mass balances for different models. In this section, the differential mass balances for growing polymer chains and their algebraic equations are included; otherwise, the modeling procedure is straightforward as demonstrated completely for the terminal model. The penultimate mechanism is summarized in Table 4, and the kinetic parameters used in simulations are shown in Table 5.

Rate of change for primary radical:

$$\frac{dC_{R_{0,0}}}{dt} = 2fk_dC_I + C_S\sum_{j=0}^{1}k_{ctSj}\mu_{0,j} - C_{R_{0,0}}\sum_{j=0}^{1}k_{pj}C_{Mj} - C_{R_{0,0}}\sum_{j=0}^{1}(k_{tdprj} + k_{tcprj})\mu_{0,j} \quad (30)$$

Table 5. Kinetic Parameters Used in Simulations/Penultimate Model

kinetic parameters	
k_d (s^{-1})	$1.58E + 15\exp(-30800/RT)$[ref 22]
	R (cal/(mol K)), T (K)
k_{p000} *(l/mol s)*	$3.16E + 7\exp(-7761.80$[ref 24]$/RT)$
k_{p111} (L/(mol s))	$2.02E + 6\exp(-5339.58$[ref 25]$/RT)$
k_{p0}, k_{p00} (L/(mol s))	k_{p000} (assumption)
k_{p1}, k_{p11} (L/(mol s))	k_{p111} (assumption)
k_{p01} (L/(mol s))	k_{p001} (assumption)
k_{p10} (L/(mol s))	k_{p110} (assumption)
k_{p001} (L/(mol s))	k_{p000}/r_{00}
k_{p110} (L/(mol s))	k_{p111}/r_{11}
k_{p101} (L/(mol s))	k_{p100}/r_{10}
k_{p010} (L/(mol s))	k_{p011}/r_{01}
k_{p100} (L/(mol s))	$k_{p000}\overline{r_{00}}$
k_{p011} (L/(mol s))	$k_{p111}\overline{r_{11}}$
k_{ctMjk}, k_{ctSj} (L/(mol s))	0
k_{tdprj}, k_{tcprj} (L/(mol s))	$8.6E + 8\exp(-1677.03/RT)$
k_{tdjk}, k_{tcjk} (L/(mol s))	$8.6E + 8\exp(-1677.03/RT)$
$r_{00} = r_{10}$	0.523[ref 23]
$r_{11} = r_{01}$	0.46[ref 23]
$\overline{r_{00}}$	0.3[ref 23]
$\overline{r_{11}}$	0.53[ref 23]

Rate of change for radical of length one with end group j:

$$\frac{dC_{R_{1,j}}}{dt} = k_{pj}C_{R_{0,0}}C_{Mj} + C_{Mj}\sum_{i=0}^{1}k_{ctMij}\mu_{0,i} - C_{R_{1,j}}\sum_{i=0}^{1}(k_{pji} + k_{ctMji})C_{Mi} - k_{ctSj}C_{R_{1,j}}C_S - C_{R_{1,j}}\sum_{i=0}^{1}(k_{tdji} + k_{tcji})\mu_{0,i} \quad (31)$$

Rate of change for radical of length two with end group ij:

$$\frac{dC_{R_{2,d}}}{dt} = k_{pij}C_{R_{1,i}}C_{Mj} - C_{R_{2,d}}\sum_{k=0}^{1}(k_{pijk} + k_{ctMjk})C_{Mk} - k_{ctSj}C_{R_{2,d}}C_S - C_{R_{2,d}}\sum_{k=0}^{1}(k_{tdjk} + k_{tcjk})\mu_{0,k} \quad (32)$$

Rate of change for radical of length ≥3 with end group kij:

$$\frac{dC_{R_{n,d}}}{dt} = \sum_{k=0}^{1}k_{pkij}C_{R_{n-1,X}}C_{Mj} - C_{R_{n,d}}\sum_{k=0}^{1}(k_{pijk} + k_{ctMjk})C_{Mk} - k_{ctSj}C_{R_{n,d}}C_S - C_{R_{n,d}}\sum_{k=0}^{1}(k_{tdjk} + k_{tcjk})\mu_{0,k} \quad (33)$$

where

$$X = \begin{cases} d/2 & \text{for } j = 0 \\ (d-1)/2 & \text{for } j = 1 \end{cases}$$

Applying QSSA, the growing polymer chain concentrations are expressed in terms of their algebraic forms. The following equations, eqs 34−36, represent the equation for the primary radical, the general equation for the two radical types of chain length 1, and the general equation for the four radical types of chain length 2, respectively.

$$C_{R_{0,0}} = \frac{2fk_dC_I + C_S\sum_{j=0}^{1}k_{ctSj}\mu_{0,j}}{\sum_{j=0}^{1}k_{pj}C_{Mj} + \sum_{j=0}^{1}(k_{tdprj} + k_{tcprj})\mu_{0,j}} \quad (34)$$

$$C_{R_{1,j}} = \frac{k_{pj}C_{R_{0,0}}C_{Mj} + C_{Mj}\sum_{i=0}^{1}k_{ctMji}\mu_{0,i}}{\sum_{i=0}^{1}(k_{pji} + k_{ctMji})C_{Mi} + k_{ctSj}C_S + \sum_{i=0}^{1}(k_{tdji} + k_{tcji})\mu_{0,i}} \quad (35)$$

$$C_{R_{2,d}} = \frac{k_{pij}C_{R_{1,i}}C_{Mj}}{\sum_{i=0}^{1}(k_{pijk} + k_{ctMjk})C_{Mk} + k_{ctSj}C_S + \sum_{k=0}^{1}(k_{tdjk} + k_{tcjk})\mu_{0,k}} \quad (36)$$

At QSSA, the following general equation is generated for the 8 cases of growing radicals of chain length ≥3 with end group ∼*kij*•:

$$C_{R_{n,d}} = \frac{k_{pkij}R_{n-1,X}C_{Mj}}{\sum_{k=0}^{1}(k_{pijk} + k_{ctMjk})C_{Mk} + k_{ctSj}C_S + \sum_{k=0}^{1}(k_{tdjk} + k_{tcjk})\mu_{0,k}} \quad (37)$$

To begin with, Figure 13 illustrates that the copolymer composition for terminal and penultimate models, at the specified kinetic parameters shown in Tables 3 and 5, respectively, are identical. Equations 38 and 39 represent copolymer composition expressions for terminal and penultimate models, respectively.

$$F_0 = \frac{r_0f_0^2 + f_0f_1}{r_0f_0^2 + 2f_0f_1 + r_1f_1^2} \quad (38)$$

where r_0 and r_1 are terminal model reactivity ratios and are defined as in Table 3, and f_i and F_i are the comonomer and copolymer composition with respect to monomer *i*, respectively.

$$F_0 = \frac{\bar{r}_0f_0^2 + f_0f_1}{\bar{r}_0f_0^2 + 2f_0f_1 + \bar{r}_1f_1^2} \quad (39)$$

where $\bar{r}_0 = r_{10}[(r_{00}f_0 + f_1)/(r_{10}f_0 + f_1)]$ and $\bar{r}_1 = r_{01}[(f_0 + r_{11}f_1)/(f_0 + r_{01}f_1)]$ and the reactivity ratios of the penultimate model are defined in Table 5.

The reactivity ratios, $\overline{r_{00}}$ and $\overline{r_{11}}$, are invisible in the copolymer composition equation and thus have no contribution to the copolymer composition. The reactivity ratios used in simulations, $r_{00} = r_{10}$ and $r_{11} = r_{01}$, cause the penultimate composition equation to revert to the Mayo−Lewis equation, eq 38, and consequently the calculated probabilities that determine monomer addition and SLD are the same for both terminal and penultimate models. Thus, the previously shown SLD of Figure 4 that represented the terminal model should equally represent the penultimate model. As a solution and to gain differentiation between models, CTD is calculated and demonstrated in Figure 14a−d for terminal and penultimate models when termination is considered either by disproportionation or by combination, respectively. The difference in CTD

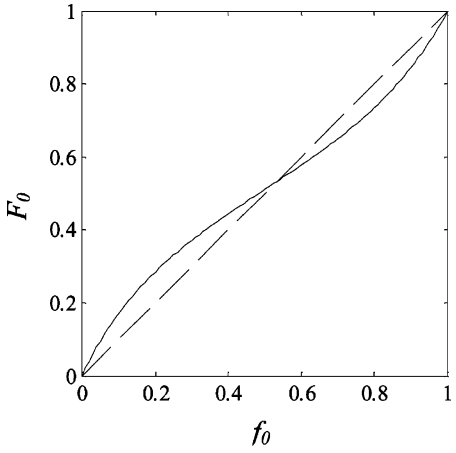

Figure 13. Copolymer composition with respect to monomer of code "0" vs comonomer composition. Solid line represents either composition calculated using kinetic parameters of Table 3 for the terminal model, eq 38, or using kinetic parameters of Table 5 for the penultimate model, eq 39.

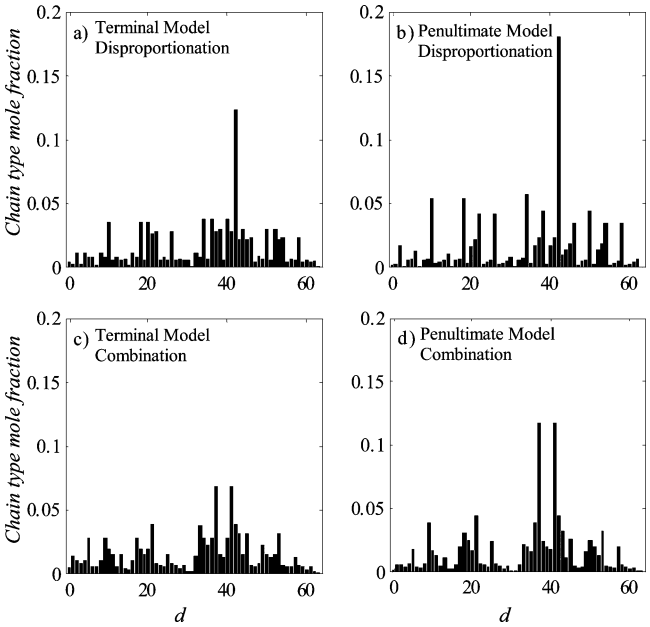

Figure 14. CTD for a chain length of 6 in a steady-state CSTR at 80 °C. $r_0 = 0.523$, $r_1 = 0.46$, and $f_0 = 0.5$: (a) terminal model/termination by disproportionation, (b) penultimate model/termination by disproportionation, (c) terminal model/termination by combination, (d) penultimate model/termination by combination.

is clear because the individual propagation rate constants are required to express the penultimate influence that alters the growing radicals propagation rate equation (37), unlike the composition equation that is dependent on reactivity ratios. For termination by disproportionation, Figure 14a,b shows that CTD distribution is qualitatively as well as quantitatively different and distinguishing between models should be possible. If a capable analytical technique is available to trace the polymer isomer concentrations for short chains, then it seems quite satisfactory to depend on CTD for model discrimination. Figure 14c,d depicts CTD for both models when termination is by combination. Both models show the same kind of trend with two most probable isomer chains at $d = 37$ and $d = 41$ of binary codes of 100101 and 101001, respectively. It is the 33% difference in concentrations of these two polymer chain in the penultimate rather than terminal model that will allow better discrimination.

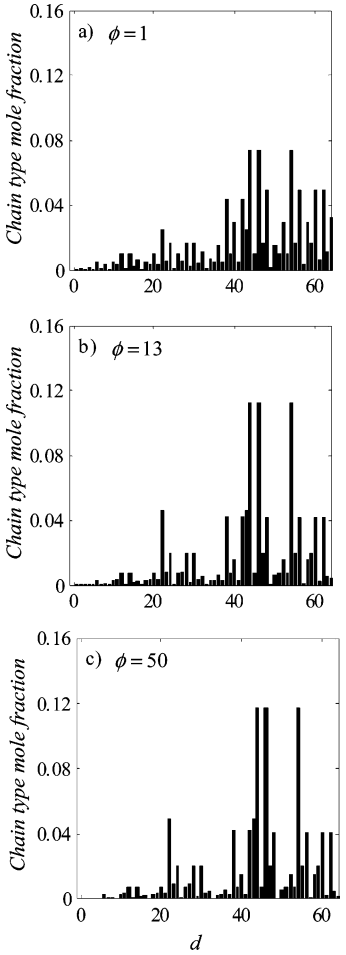

Figure 15. CTD for a chain length of 6 in a steady-state CSTR at 80 °C. $r_0 = 0.523$, $r_1 = 0.46$, $f_0 = 0.3$, and for chemically controlled, by combination, termination. (a) $\phi = 1$, (b) $\phi = 13$, (c) $\phi = 50$.

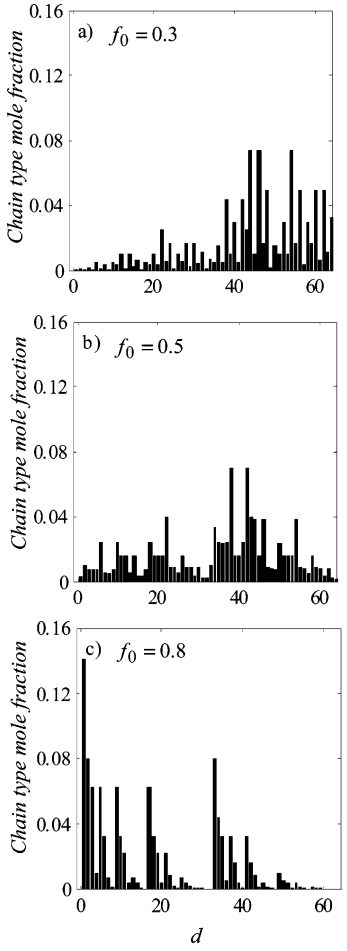

Figure 16. CTD for a chain length of 6 in a steady-state CSTR at 80 °C. $r_0 = 0.523$, $r_1 = 0.46$, and for diffusion-controlled, by combination, termination. (a) $f_0 = 0.3$, (b) $f_0 = 0.5$, (c) $f_0 = 0.8$.

Case Study: Styrene/Methyl Methacrylate; Termination Mechanism Differentiation. Buback et al.[35] outlined major pieces of evidence for free radical termination being diffusion-controlled whether termination is dominated by combination or disproportionation. They also noted that for unusual systems suspicions sometimes arise that termination is chemically controlled, but all the general evidence suggests that termination in free radical polymerizations should be regarded as diffusion-controlled until proven otherwise.

For the styrene/methyl methacrylate system, Fukuda et al.[23] found that previous results indicating large composition-dependent values of the cross-termination factor, $\phi = k_{t01}/(k_{t00}k_{t11})^{0.5}$, are erroneous and that the termination rate constants are well represented by the chemical model with $\phi = 1$ for $r_0 = 0.523$ and $r_1 = 0.46$ as well as by the diffusion model. Then, they concluded that that the choice between termination models for this case is difficult on the basis of numerical comparison alone, and in view of the body of evidence, the diffusion model seems to be more realistic. In contrast, Walling[36] and Chiang et al.[37] studied the styrene/methyl methacrylate system and reported that $\phi = 13$ for $r_0r_1 = 0.24$. They mentioned that diffusion model is more realistic for some copolymerization systems such as methyl methacrylate/vinyl acetate, but it cannot account for the behavior of styrene/methyl methacrylate because termination rate constant values in the individual homopolymerizations are almost similar, but the rate of copolymerization is relatively depressed when the reacting mixture contains more than about 0.2 mole fraction of styrene.

In this regard, CTD results can be of help to differentiate between chemically and diffusion-controlled termination and can assist in detecting the influence of ϕ on the copolymer microstructure. Figures 15a−c demonstrates the influence of the chemical model when $\phi = 1$, $\phi = 13$, $\phi = 50$ and when termination is by combination at $f_0 = 0.3$, respectively. CTD responds to change in ϕ, but as it increases less effect is noticed. Increasing ϕ means that cross-termination is favored over homotermination, and therefore as ϕ gets more dominating, CTD gets fixed but that should not mean that chain type concentrations are fixed. Figure 15a,b shows that the argument whether ϕ =1 or 13 could be resolved by comparing CTD that is quite distinctive. In contrast, Figure 16a−c shows CTD when termination is diffusion-controlled, $k_t = k_{t00} = k_{t11} = k_{t01}$, for $f_0 = 0.3$, 0.5, and 0.8, respectively, and when termination is by combination. CTD is different as copolymer composition changes and behaves as described for cases when termination is by disproportionation of Figure 8a−c. Note that for all discussed examples in this work an ideal diffusion-controlled termination is considered where $k_t = F_0k_{t00} + F_1k_{t11}$, unless mentioned otherwise. Despite the differences between CTD at various comonomer compositions, an agreement with findings of Fukuda et al.[23] can be seen for similar CTD of the chemically controlled termination at $\phi = 1$ and the diffusion-controlled termination, Figures 15a and 16a, respectively. Such a result is expected because radical type distribution is affected by the individual propagation rate constants; then what differentiates between CTD at either termination mechanism are

CDV

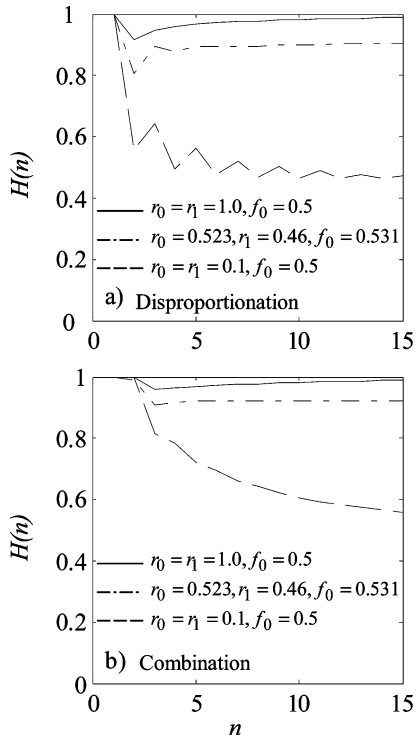

Figure 17. Modified Shannon entropy, $H(n)$, for chain length up to 15 units. Solid line: $(r_0,r_1) = (1.0, 1.0)$ and $f_0 = 0.5$; dash−dotted line: $(r_0,r_1) = (0.523, 0.46)$ and azeotropic composition $f_0 = F_0 = 0.531$; dashed line: $(r_0,r_1) = (0.1, 0.1)$ and $f_0 = 0.5$. (a) Termination by disproportionation, (b) termination by combination.

the individual termination rate constants, which for this case are all equal.

Complexity in CTD. After collecting complete information about a particular system, the next step would be to distinguish uniform distributions and detect particular regularities or patterns that can represent the behavior of that system.

The average degree of organization of CTD is implicit in the Shannon entropy[15] which is a measure of complexity or randomness. The modified (normalized) Shannon entropy of n order, $H(n)$, is based on the probability distribution, CTD in our case, of chain sequences with length n and is defined as

$$H(n) = -\frac{1}{\log_2 N}\sum_i P_i \log_2(P_i) \qquad (40)$$

where N is the total number of chain types of length n, i is indexing chain sequences of given length n, and P_i is the probability of the ith chain sequence. For random chain sequences we should have $H(n) = 1$; otherwise, it should be $0 \le H(n) \le 1$ and lower $H(n)$ implies more deterministic structure. Note that there is no theoretical rule to determine which chain length n is sufficient or best for observing particular patterns, in case they exist.

Figure 17a,b shows the modified Shannon entropy, $H(n)$, for chain length up to 15 units, at the alternating, azeotrope and random cases where Figure 17a is when termination by disproportionation and Figure 17b is when termination by combination. The system shows appreciative fluctuations in entropy of short chains which can serve as an indicator of differences in chain mole fractions as well as in termination mode effects. It is these differences in entropy of short polymer chains that suggest a wealth of knowledge about the system if unfolded by using the digital encoding technique.

As chain length increases, the entropy of the system tends to be fixed. Therefore, chain lengths of 15−20 are suggested to be sufficient to extract precise information about the copolymerization system.

Finally, the fixed entropy of the system suggests that there maybe an evolution pattern of polymeric chains that fixes the order in the system and can make its CTD predictable from short chains. Work is developed and will be published to mathematically validate the ability of short chains to represent longer polymer chains by predicting the complete distributions of these longer chains from "short-chain blueprints" and by determining the most dominant chain microstructures that are responsible for the polymer properties at high chain length.

Conclusions

The mathematical model equations of "digital encoding of polymer chains" were developed for a free radical copolymerization obeying the terminal model in a dynamic isothermal CSTR, but their solution was restricted to a steady-state operation. The proposed digital encoding technique provided a new descriptive method for all polymer chain types including their polymeric isomers which were not previously possible. This powerful technique is a suitable method for the graphical representation of encoded sequence length (SLD) and chain type (CTD) distributions which allow not only the ability to distinguish between polymer isomers but also to map the polymerization process at various conditions based on short chains analysis. This mapping will provide a better tool for model discrimination, termination mechanism, and mode differentiation and importantly the better design and control of copolymer microstructure in terms of architecture, functionality, and composition. Further application of this method accompanied by better analytical techniques could lead to better tailored polymeric structures with advanced properties.

References and Notes

(1) Debling, J. A.; Teymour, F. *Macromol. Symp.* **2002**, *182*, 195−207.
(2) Holley, R. W. *Nobel Lectures*; Physiology or Medicine 1963−1970; Elsevier Publishing Co.: Amsterdam; 1972; pp 324−338.
(3) Crutchfield, J. P.; Packard, N. H. *Physica D* **1983**, *7*, 201−223.
(4) Tang, X. Z.; Tracy, E. R.; Boozer, A. D.; deBrauw, A.; Brown, R. *Phys. Rev. E* **1995**, *51*, 3871−3889.
(5) Lehrman, M.; Rechester, A. B.; White, R. B. *Phys. Rev. Lett.* **1997**, *78*, 54−57.
(6) Finney, C. E. A.; Green, J. B.; Daw, C. S. *SAE Paper* **1998**, *No. 980624*.
(7) Daw, C. S.; Finney, C. E. A.; Kennel, M. B. *Phys. Rev. E* **2000**, *62*, 1912−1921.
(8) Shull, K. R. *Macromolecules* **2002**, *35*, 8631−8639.
(9) Greszta, D.; Matyjaszewski, K.; Pakula, T. *T. Polym. Prepr. (Am. Chem. Soc., Div. Polym. Chem.)* **1997**, *38*, 709−710.
(10) Matyjaszewski, K.; Greszta, D.; Pakula, T. T. *Polym. Prepr. (Am. Chem. Soc., Div. Polym. Chem.)* **1997**, *38*, 707−708.
(11) Greszta, D. Ph.D. Thesis, Carnegie Mellon University, 1997.
(12) Zhang, M.; Ray, W. H. *J. Appl. Polym. Sci.* **2002**, *86*, 1630−1662.
(13) Zhang, M.; Ray, W. H. *Ind. Eng. Chem. Res.* **2001**, *40*, 4336−4352.
(14) Zhang, M. Ph.D. Thesis, University of Wisconsin−Madison, 2001.
(15) Shannon, C. E. *Bell Syst. Technol. J.* **1948**, *27*, 379−423, 623−656.
(16) Dotson, N. A.; Galvan, R.; Lawrence, R. A.; Tirrell, M. *Polymerization Process Modeling*; VCH Publishers: New York, 1996.
(17) Koenig, J. L. *Spectroscopy of Polymers*, 2nd ed.; Elsevier Science: New York, 1999.
(18) Koenig, J. L. *Chemical Microstructure of Polymer Chains*; John Wiley & Sons: New York, 1980.
(19) Tabash, R.; Teymour, F. *Chem. Eng. Sci.* **2004**, *59*, 22−23, *ISCRE18*, 5129−5137.
(20) Tabash, R.; Teymour, F. AICHE Meeting 2003, San Francisco, 91e.
(21) Ray, W. H. *J. Macromol. Sci., Rev. Chem.* **1972**, *C8*, 1−56.
(22) Pinto, J. C.; Ray, W. H. *Chem. Eng. Sci.* **1995**, *50*, 715−736.

(23) Fukuda, T.; Ma, Y.; Inagaki, H. *Macromolecules* **1985**, *18*, 17−26.
(24) Buback, M.; Gilbert, R. G.; Hutchinson, R. A.; Klumperman, B.; Kuchta, F. D.; Manders, B. G.; O'Driscoll, K. F.; Russell, G. T.; Schweer, J. *Macromol. Chem. Phys.* **1995**, *196*, 3267−3280.
(25) Beuermann, S.; Buback, M.; Davis, T. P.; Gilbert, R. G.; Hutchinson, R. A.; Olaj, O. F.; Russell, G. T.; Schweer, J.; van Herk, A. M. *Macromol. Chem. Phys.* **1997**, *198*, 1545−1560.
(26) Theil, M. H. *J. Polym. Sci., Polym. Chem.* **1983**, *21*, 633−634, 1558.
(27) Flory, P. J. *Principles of Polymer Chemistry*, Cornell University Press: London, 1953.
(28) Odian, G. *Principles of Polymerizations*, 3rd ed.; John Wiley & Sons: New York, 1991.
(29) Hill, D. J. T.; O'Donnell, J. H.; O'Sullivan, P. W. *Macromolecules* **1982**, *15*, 960−966.
(30) O'Driscoll, K. F.; Davis, T. P. *J. Polym. Sci., Part C* **1989**, *27*, 417−420.
(31) Maxwell, I. A.; Aerdts, A. M.; German, A. L. *Macromolecules* **1993**, *26*, 1956−1964.
(32) Ma, Y.; Fukuda, T.; Inagaki, H. *Macromolecules* **1985**, *18*, 26−31.
(33) Fukuda, T.; Ma Y.; Kubo, K.; Inagaki, H. *Macromolecules* **1991**, *24*, 370−375.
(34) Fukuda, T.; Ma, Y.; Inagaki, H. *Polym. Bull. (Berlin)* **1983**, *10*, 288−290.
(35) Buback, M.; Egorov, M.; Gilbert, R. G.; Kaminsky, V.; Olaj, O. F.; Russell, G. T.; Vana, P.; Zifferer, G. *Macromol. Chem. Phys.* **2002**, *203*, 2570−2582.
(36) Walling, C. *Free Radicals in Solutions*; Wiley & Sons: New York, 1957.
(37) Chiang, S. S. M.; Rudin, A. *J. Macromol. Sci., Chem.* **1975**, *A9*, 237−256.

MA051417Y